Application of Tuning Fork Sensors for In-situ Studies of Dynamic Force Interactions Inside Scanning and Transmission Electron Microscopes

ISSN 1392–1320 MATERIALS SCIENCE (MEDŽIAGOTYRA). Vol. 18, No. 2 2012

Application of Tuning Fork Sensors for In-situ Studies of Dynamic Force Interactions Inside Scanning and Transmission Electron Microscopes

Jana ANDZANE [1], Raimonds POPLAUSKS [1], Juris PRIKULIS [1], Rünno LÕHMUS [2], Sergei VLASSOV [2], Sergey KUBATKIN [3], Donats ERTS [1 *]

[1] *Institute of Chemical Physics, University of Latvia, Raiņa bulvāris 19, LV-1586 Rīga, Latvia*
[2] *Institute of Physics, University of Tartu, Riia 142, 51014 Tartu, Estonia*
[3] *Department of Microtechnology and Nanoscience, Chalmers University of Technology, SE-412 96 Göteborg, Sweden*

crossref http://dx.doi.org/10.5755/j01.ms.18.2.1927

Received 14 September 2011; accepted 17 October 2011

Mechanical properties of nanoscale contacts have been probed in-situ by specially developed force sensor based on a quartz tuning fork resonator (TF). Additional control is provided by observation of process in scanning electron microscope (SEM) and transmission electron microscope (TEM). A piezoelectric manipulator allows precise positioning of atomic force microscope (AFM) probe in contact with another electrode and recording of the TF oscillation amplitude and phase while simultaneously visualizing the contact area in electron microscope. Electrostatic control of interaction between the electrodes is demonstrated during observation of the experiment in SEM. In the TEM system the TF sensor operated in shear force mode: Use of TEM allowed for direct control of separation between electrodes. New opportunities for in situ studies of nanomechanical systems using these instruments are discussed.
Keywords: friction, nanomechanics, tuning fork, microscopy, NEMS.

1. INTRODUCTION

Atomic force microscopes (AFM) are widely used for morphology, force interactions, electrical and optical measurements on local scale in material science, nanotechnologies, biology and other areas. Development of AFM compatible with transmission electron microscopes (TEM) [1 – 3] open new opportunities for investigation of nanocontacts in-situ. Several cantilever deflection sensing systems are available for static force detection inside TEM instead of the traditional optical method, e. g. direct imaging of the cantilever displacement with a known force constant in TEM [2] or use of micromachined capacitive force sensor [4]. The functionality of AFM and range of suitable samples can be extended further by integration of AFM in scanning electron microscopes (SEM) capable of hosting even relatively bulky optical cantilever deflection detector [3, 4]. The TEM-AFM and SEM-AFM systems presented in this article utilize compact tuning fork (TF) force sensors and enable noncontact probing and studies of dynamic interactions such as friction, allowing direct visualization of contact area and mechanical oscillations.

Application of TF sensors in AFM has gained popularity because it offers an inexpensive alternative to optical detection of cantilever oscillation, with high force constant and easy control where only electrical connections are available, e. g., vacuum systems and low temperature setups. In addition, the high rigidity of TF sensors allow force detection with small oscillation amplitude, which results in higher imaging resolution [5].

With its small size (only few mm across) the TF is particularly well suited for instruments inside electron microscopes, where space is scarce. In scanning probe applications TF were used as shear force sensors and employed for distance control in near-field scanning optical microscopy [6]. It has been shown that TF can be used as sensors for noncontact mode AFM [7] showing atomic resolution [8], biological applications [9] and even for scanning single electron transistor microscopy [11].

Studies of force interactions in nanocontacts are important for fundamental understanding of friction, tribology and related phenomena. Despite the experimental and theoretical simplicity of friction on macroscopic scale the underlying nature of contact and noncontact interactions in nanometer sized systems is still actively debated [2, 10, 11]. Several mechanisms contribute to noncontact friction force, such as electromagnetic fluctuations, electronic and phonon excitations [12], fluctuation of thermal fields [13], adsorbed liquid layer on the surface [14]. Experimental verification of theoretical model systems is difficult since the interaction is sensitive to exact chemical composition of interacting materials, presence of any process residuals as well as precise definition of contact geometry.

Due to the tiny size of the contacts, shape variations during operation may be caused by wear, which is a key factor to reliability of nanomechanical devices in practical applications [15].

While sampling of phase or amplitude of the TF oscillation is sufficient for distance regulation in SPM, additional force control parameters are required for development of nanoelectromechanical systems (NEMS), e.g. switching devices [16], storage systems [17] or in-situ nanoscale experiments in material science. Proposed NEMS relay on subtle balance between the local elasticity, friction, electrostatic and van der Waals forces.

Due to complexity of theoretical models and difficulty to reproduce exact conditions in measurements, experimental tools are required for express tests and rapid

*Corresponding author. Tel.: +370-6703385; fax.: +370-6703384.
E-mail address: *donats.erts@lu.lv* (D. Erts)

development of NEMS prototypes. Here we present and compare two variations of TF based experimental methods, which allow controlling and monitoring various combinations of device parameters, such as contact geometry, applied electrostatic field and oscillation amplitude.

An important advantage of presented technique is that attachment of sample materials to the TF sensors does not require sophisticated microfabrication techniques such as lithography.

2. EXPERIMENTAL

TEM holder with integrated TF has been developed for transmission electron microscope Philips 301. Experiments were performed at room temperature. The electronics module was developed for TF excitation followed by amplitude and phase signal detection. Home built controller and acquisition electronics and software were used in experiments.

The design of the TEM holder is similar to what has been used in [2]. An integrated piezo tube scanner was used for precise positioning of the sample. A schematic diagram and photograph of the TEM holder with the TF sensor is shown in Fig. 1. Oscillation of the TF was driven by application of sinusoidal voltage on one electrode and current was measured at other electrode of the TF using an inverting I-V converter. In order to increase scanning speed for AFM imaging applications typically one prong of the TF is glued to a supporting structure. This reduces quality factor to approximately 5000 [7] while for standard TF the quality factor can be much higher. In our device both TF prongs are free and AFM tip glued to one prong of TF [18] as shown in Fig. 2. After hardening of the glue the supporting chip and cantilever were removed. Focused ion beam cutting can be used to mark the exact breaking position. While TEM offers the best resolution of imaging, initial alignment of the sample and probe is a delicate process, which requires skills and patience.

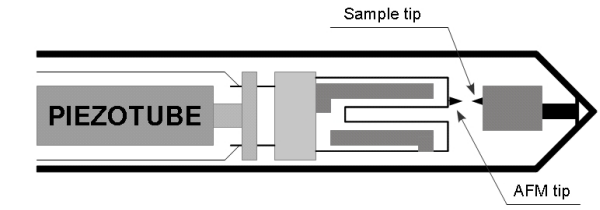

a

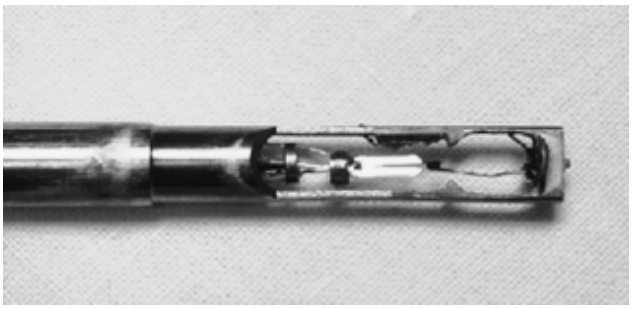

b

Fig. 1. Schematic diagram (a) and photograph (b) of TEM holder with TF force sensor

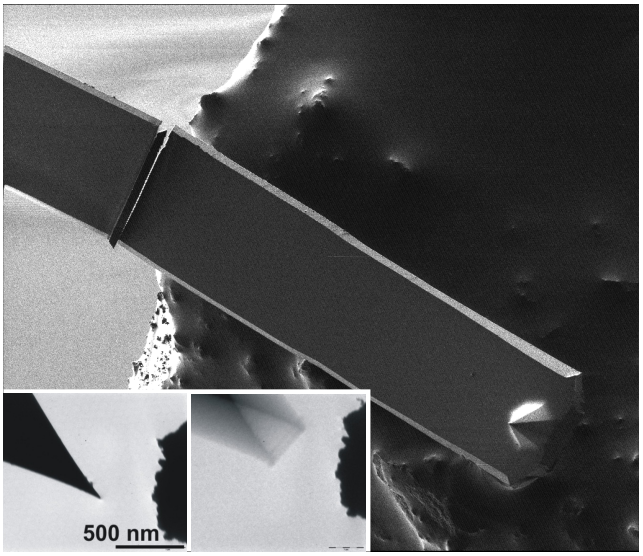

Fig. 2. SEM image of an AFM probe glued to the end of a TF. Insets: TEM images of the AFM probe at rest and oscillating at TF resonance frequency

For improved flexibility and additional functionality a similar system was built for dynamic force studies inside SEM. In this case a conductive AFM tip was glued to a standard quartz TF with a nominal resonance frequency $f_0 = 32.768$ kHz so that electrical contact was formed with the TF electrodes. In such configuration one TF electrode together with the AFM probe can be attached to the common electrical ground. This eliminates accumulation of charge in SEM experiments and allows control of the contact gap potential by simple DC voltage application at the sample electrode. Both sides of the contact were attached to a manipulator (SmarAct 13D) inside a SEM (Hitachi S-4800). The manipulator allows accurate placement of the probes and estimate of the contact geometry. Instead of inverting amplifier, which was used in TEM case, a noninverting configuration of an operational amplifier (AD549JH) as shown in Fig. 3. was built. The key feature of this setup is that all elements have a well defined potential relative to the common ground. In order to minimize any cable capacitances, the amplifier was placed in the vicinity of the TF inside the SEM vacuum chamber. The output voltage is then determined by $U_{out} = U_{in}(1 + R/Z)$, where $R = 100$ kΩ is the resistance of the feedback resistor and Z is the frequency dependent complex impedance of the TF. The feedback regulates the voltage on the TF electrodes always to be constant U_{in} independently from the resonance current. The mechanical oscillation can be observed as a blur on the right side electrode in Fig. 4, d. For this particular experiment a value of $U_{in} = 7$ mV was used. Phase and amplitude of the TF oscillation was extracted using lock-in amplifier (Nanonis OC4). A DC voltage with current limiter was applied between the contact electrodes using Keithley 6430 sourcemeter. In the ideal case the lateral TF oscillations would be normal to the applied electric field. However, deviations are caused by drift and projection limits of the imaging system. Similarly, a significant normal component of the oscillations can be observed in the TEM case (Fig. 4, a, b).

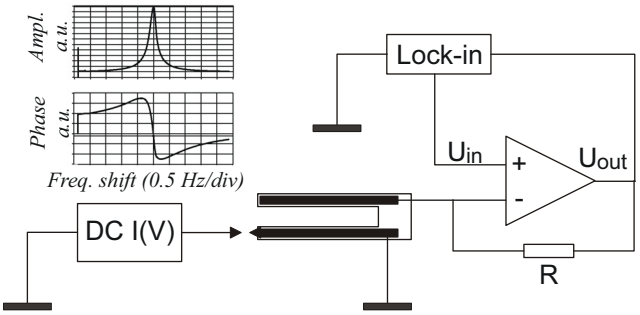

Fig. 3. Electrical connection diagram of the experimental setup inside SEM. Inset: Amplitude and phase of U_{out} with center frequency $f_0 = 32.764$ kHz (value for TF with attached conductive probe) recorded in air

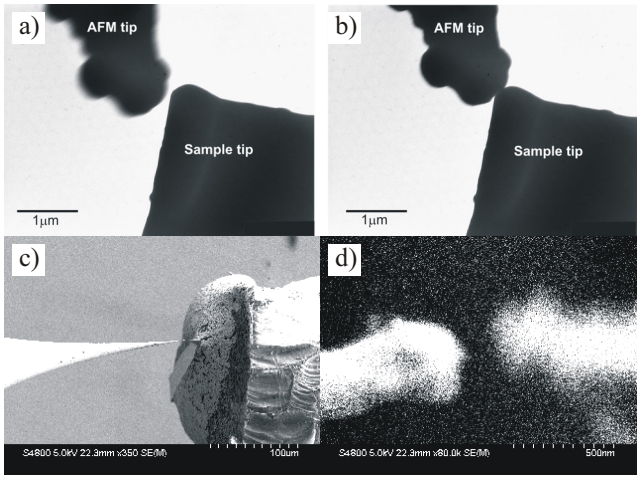

Fig. 4. Electron microscopy images of contact area. In TEM experiments tip of etched Au wire was used: before contact (a); in contact (b); conductive AFM probe glued to a TF approaching an etched tungsten electrode in SEM experiments (c); high magnification image of the contact area (d)

The gap between the electrodes was reduced with ~(0.5 – 2) nm steps using scan move of the piezopositioner during which the amplitude and phase were recorded. The exact time between the steps cannot be determined due to limitations of the controller operating system, and is estimated to be within 20…100 ms range.

3. RESULTS AND DISCUSSION

Fig. 5, a, shows the resonance peak of the TF with mounted AFM tip used in TEM experiments. After mounting the tip on one of the prongs the quality factor of the TF resonator remains high (7000 – 9000) and the resonance frequency is decreased only by 2 % – 3 % of its initial value.

The hysteresis observed in approach and withdrawal curves (Fig. 5, b, c) could originate from plastic deformations of the soft Au sample even if no physical contact has been established, or presence of adsorbed liquid on the contact surface. However, it should be mentioned, that the recorded amplitude and phase values do not represent steady state of oscillations for given conditions. The high quality resonator requires time $\tau \approx 1/\Delta f$ to respond to changing conditions, where Δf is the width of the resonance peak. However, the operating speed can be significantly improved when distance regulation feedback loop is turned on [22].

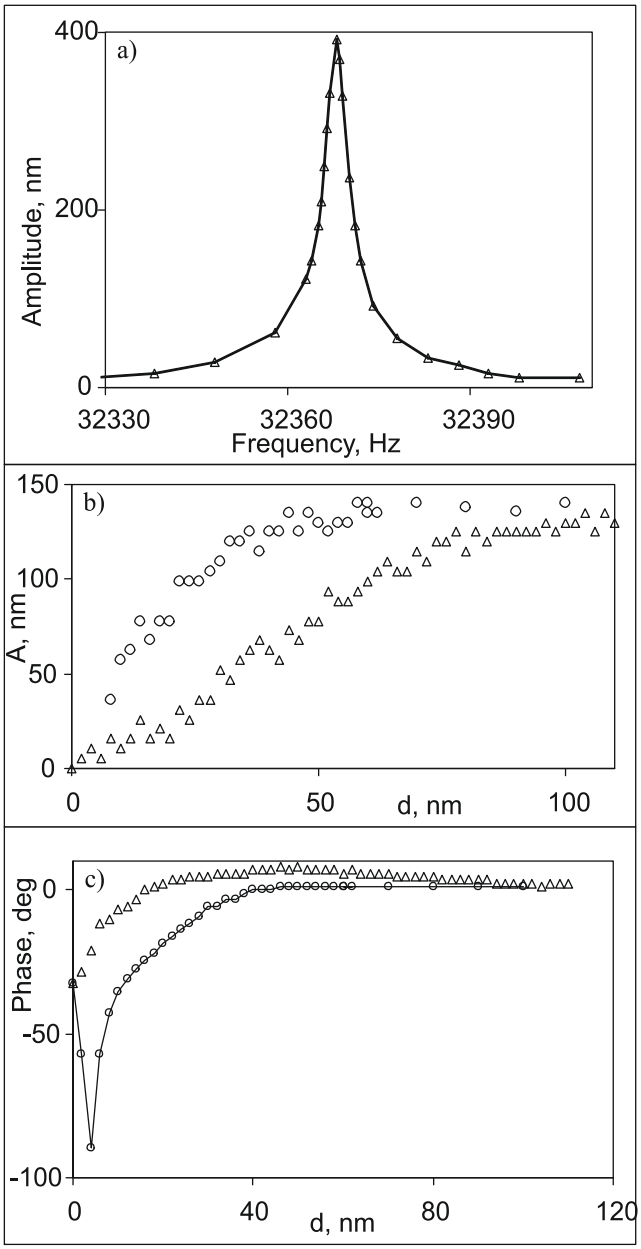

Fig. 5. Amplitude resonance curve for the probe used in TEM experiments (a). The tuning fork Q factor was 8100. Amplitude (b) and phase dependence (c) on distance in approach (circles) – withdrawal (triangles) curves

For demonstration of the SEM setup and analysis of the role of electrostatic interaction in shear force detection we used an electrochemically etched tungsten tip [19] and a conductive AFM probe as shown in Fig. 4, c, d. A series of amplitude and phase curves were recorded during approach and withdrawal of the contacts at various gap potentials. The applied voltages were between 0 V and 20 V. During recording of the curves the current protection level of the voltage source, which was set to set to 100 nA, was never reached even in mechanical contact, most likely due to presence of oxide layer on the W tip [19]. After recording the series, severe force was applied to the electrodes in order to check the electrical connections. The established Ohmic contact between the two electrodes

eventually caused melting of the W tip and damage of the probe.

Fig. 6 shows the amplitude and phase of the U_{out} signal during approach ("go") and withdrawal ("return") of the contact. In order to compensate for slow mechanical drift between recordings, the data in Fig. 6 was aligned so that the zero position on horizontal axis was at the point where amplitude has dropped to 50 % of the free oscillation case during approach. A clear hysteresis in amplitude of the approach-withdrawal cycle can be observed. It should be noted that at full contact, when the oscillations are completely damped the U_{out} drops to the level of U_{in} instead of zero due to constant 1 in the amplifier transfer function. Similarly the phase of the complex R/Z signal is superimposed to that of U_{in}. The width of the hysteresis varied between 20 nm and 60 nm in the approach-withdrawal curves of the amplitude. However, there is no obvious correlation between the amplitude signal and the applied gap voltage. Several factors may contribute to the dynamic behavior of the oscillation amplitude during approach and withdrawal. The scatter of the hysteresis width may be due to relative drift of the electrodes in lateral direction or plastic deformation of the probe. In addition the transition time from free oscillations to full contact and back happens within the timescale of seconds which is comparable to the inverse of the resonance peak width of approximately 1 Hz.

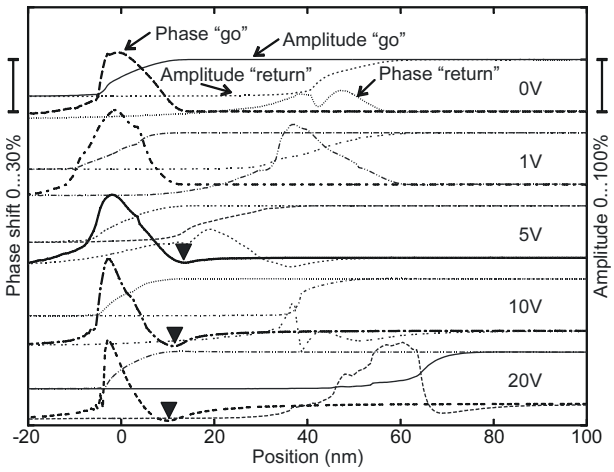

Fig. 6. Amplitude and phase of the recorded signal measured as a function of the sensor position at various gap voltages

In contrast to amplitude signal the phase clearly exhibits features related to the gap voltage. When sufficient potential is applied to the W electrode, the phase signal gradually decreases during approach, reaches its minimum indicated with ▼ in Fig. 6 and then rapidly changes in a manner similar to the case of zero bias voltage. The changes in the phase signal start at much greater distance when higher DC voltage is applied between the electrodes. This behavior can be expected since the electrostatic force has the longest range of all interactions between the two contacts [20]. As can be deduced from the phase curve in inset of Fig. 3, the presence of gap voltage reduces the resonance frequency of the system and consequently causes the observed minimum of the phase signal during approach. A further analysis is required to study this behavior in detail, however this example demonstrates a potential application area of such nanocontact systems, namely voltage controlled oscillators, which is an essential part of high frequency communication systems. We note that the frequency shift in the experiment was not caused by any change of mass of the TF probe since the process was fully reversible. The 1 V bias curve, where no minimum can be observed, was recorded between the 10 V and 20 V cases.

Finally, we inspect the phase response during withdrawal. The occasional beats in the signal indicate interference between oscillators with slightly different frequencies. This behavior can be understood as the TF swings into resonance under changing conditions, namely the electrodes undergo a transition from contact to noncontact interaction.

3. CONCLUSIONS

In this paper we presented two alternative designs of electron microscope compatible manipulation and probing systems, which use quartz TF as the force sensor. Compared to conventional cantilevers, the main advantages of TF sensor is its self sensing capability, i. e., no optical components are required for measurement of the distance [21]. TEM observation of samples allows a direct measurement of sample separation in noncontact experiments whereas this requires elaborate methods, such as calibrated tunneling current feedback systems when no visualization is possible. Similarly, the TF oscillation amplitude is determined by direct measurement. Usually, this requires a dissipated current calibration using interferometer methods. TF oscillation amplitude was measured directly inside TEM and calibrated vs. measured electrical signal. When the gap between the probe and sample is reduced the TF oscillation is damped by lateral (friction) forces although normal component cannot be excluded. The relatively large sensing distance (>50 nm) indicates presence of long range electrostatic interaction which, was studied in more detail using SEM setup.

We have demonstrated a design of a TF based sensor for measurements of dynamic forces in nanometer sized contacts with variable gap potential inside SEM. Most information can be extracted from the oscillation phase signal, which shows frequency shift caused by applied electrostatic potential. This could be used as nanoelectromechanical voltage controlled oscillator (VCO) element. Other possible applications of this method include studies of semiconductor materials where probe induced change of carrier concentration may extend the applicability of in-situ manipulation techniques [22] and provide higher functionality to NEMS devices.

Acknowledgments

This work has been supported by Latvian National Program in Materials Science, Latvia Council of Science, European Science Foundation Fanas program "Nanoparma", Estonian Science targeted projects SF 01800058s07, and Estonian Science Foundation under grant No 8377.

REFERENCES

1. **Erts, D., Lõhmus, A., Lõhmus, R., Olin, H.** Instrumentation of STM and AFM Combined with Transmission Electron Microscope *Applied Physics A* 72 2001: pp. S71 – S74.
2. **Erts, D., Lõhmus, A., Lõhmus, R., Olin, H., Pokropivny, A., Ryen, L., Svensson, K.** Force Interactions and Adhesion of Gold Contacts Using a Combined Atomic Force Microscope and Transmission Electron Microscope *Applied Surface Science* 188 (3 – 4) 2002: pp. 460 – 466.
3. **Kizuka, T., Ohmi, H., Sumi, T., Kumazawa, K., Deguchi, S., Naruse, M., Fujisawa, S., Sasaki, S., Yabe, A., Enomoto, Y.** Simultaneous Observation of Millisecond Dynamics in Atomistic Structure, Force and Conductance on the Basis of Transmission Electron Microscopy *Japanese Journal of Applied Physics* 40 2001: pp. L170 – L173.
4. **Nafari, A., Danilov, A., Rödjegård, H., Enoksson, P, Olin, H.** A Micromachined Nanoindentation Force Sensor *Sensors and Actuators A* 123 – 124 2005: pp. 44 – 49.
5. **Troyon, M., Lei, H., Wang, Z., Shang, G. A.** Scanning Force Microscope Combined with a Scanning Electron Microscope for Multidimensional Data Analysis *Microscopy Microanalysis Microstructures* 8 (6) 1997: pp. 393 – 402.
6. **Fukushima, K., Kawai, S., Saya, D., Kawakatsu, H.** Measurement of Mechanical Properties of Three-dimensional Nanometric Objects by an Atomic Force Microscope Incorporated in a Scanning Electron Microscope *Review of Scientific Instruments* 73 (7) 2002: pp. 2647 – 2650.
7. **Heyde, M., Kulawik, M., Rust, H.-P., Freund, H.-J.** Frequency-modulated Atomic Force Spectroscopy on NiAl(110) Partially Covered with a Thin Alumina Film *Physical Review B* 73 (12) 2006: p. 125320.
8. **Karraï, K. Grober, R. D.** Piezo-electric Tuning Fork Tip-sample Distance Control for Near Field Optical Microscopes *Ultramicroscopy* 61 (1 – 4) 1995: pp. 197 – 205.
9. **King, G. M., Lamb, J. S., Nunes, G.** Quartz Tuning Forks as Sensors for Attractive-mode Force Microscopy under Ambient Conditions *Applied Physics Letters* 79 (11) 2001: pp. 1712 – 1714. http://dx.doi.org/10.1063/1.1402960
10. **Giessibl, F. J.** Atomic Resolution on Si(111)-(7×7) by Noncontact Atomic Force Microscopy with a Force Sensor Based on a Quartz Tuning Fork *Applied Physics Letters* 76 (11) 2000: pp. 1470 – 1472.
11. **King, G. M., Nunes, G.** Attractive-mode Force Microscope for Investigations of Biomolecules under Ambient Conditions *Review of Scientific Instruments* 72 (11) 2001: pp. 4261 – 4265. http://dx.doi.org/10.1063/1.1406927
12. **Brenning, H., Kubatkin, S., Erts, D., Kafanov, S. G., Bauch, T., Delsing, P. A.** Single Electron Transistor on an Atomic Force Microscope Probe *Nano Letters* 6 (5) 2006: pp. 937 – 941.
13. **Gao, J., Luedtke, W. D., Gourdon, D., Ruths, M., Israelachvili, J. N., Landman, U.** Frictional Forces and Amontons' Law: From the Molecular to the Macroscopic Scale *The Journal of Physical Chemistry B* 108 (11) 2004: pp. 3410 – 3425.
14. **Mo, Y., Turner, K. T., Szlufarska, I.** Friction Laws at the Nanoscale *Nature* 457 (26) 2009: pp. 1116 – 1119.
15. **Dedkov, G. V.** Nanotribology: Experimental Facts and Theoretical Models *Physics-Uspekhi* 43 (6) 2000: pp. 541 – 572.
16. **Zurita-Sánchez, J. R., Greffet, J.-J., Novotny, L.** Friction Forces Arising from Fluctuating Thermal Fields *Physical Review A* 69 2004: p. 022902.
17. **La Rosa, A., Cui, X., McCollum, J., Li, N., Nordstrom, R.** The Ultrasonic/Shear-force Microscope: Integrating Ultrasonic Sensing into a Near-field Scanning Optical Microscope *Review of Scientific Instruments* 76 2005: p. 093707.
18. **Bhushan, B.** Nanotribology and Nanomechanics of MEMS/NEMS and BioMEMS/BioNEMS Materials and Devices *Microelectronics Engineering* 84 (3) 2007: pp. 387 – 412.
19. **Andzane, J., Prikulis, J., Dvorsek, D., Mihailovic, D., Erts, D.** Two-terminal Nanoelectromechanical Bistable Switches Based on Molybdenum-sulfur-iodine Molecular Wire Bundles *Nanotechnology* 21 (12) 2010: p. 125706.
20. **Tsuchiya, Y., Takai, K., Momo, N., Nagami, T., Yamaguchi, S., Shimada, T., Mizuta, H., Oda, S.** Nanoelectromechanical Nonvolatile Memory Device Incorporating Nanocrystalline Si Dots *Journal of Applied Physics* 100 2006: p. 094306. http://dx.doi.org/10.1063/1.2360143
21. **Rozhok, S., Chandrasekhar, V.** Application of Commercially Available Cantilevers in Tuning Fork Scanning Probe Microscopy (SPM) Studies *Solid State Communications* 121 (12) 2002: pp. 683 – 686. http://dx.doi.org/10.1016/S0038-1098(02)00035-2
22. **Grober, R. D., Acimovic, J., Schuck, J., Hessman, D., Kindlemann, P. J., Hespanha, J., Morse, A. S., Karrai, K., Tiemann, I., Manus, S.** Fundamental Limits to Force Detection Using Quartz Tuning Forks *Review of Scientific Instruments* 71 2000: pp. 2776 – 2780.
23. **Oliva, A. I., Romero, A., Peña, J. L., Anguiano, E., Aguilar, M.** Electrochemical Preparation of Tungsten Tips for a Scanning Tunneling Microscope *Review of Scientific Instruments* 67 1996: p. 1917.
24. **Israelachvili, J. N.** Intermolecular and Surface Forces. 2nd ed. San Diego, CA: Academic Press, 1992.
25. **Andzane, J., Petkov, N., Livshits, A. I., Boland, J. J., Holmes, J. D., Erts, D.** Two-Terminal Nanoelectromechanical Devices Based on Germanium Nanowires *Nano Letters* 9 (5) 2009: pp. 1824 – 1829.
26. **Spence, J. C. N.** A Scanning Tunneling Microscope in a Side-entry Holder for Reflection Electron Microscopy in the Philips EM400 *Ultramicroscopy* 25 (2) 1988: pp. 165 – 169.

Presented at the 13-th International Conference-School
"*Advanced Materials and Technologies*"
(*August 27–31, 2011, Palanga, Lithuania*)